May 1999

Photodetachment of Na^-

Chien-Nan Liu
University of Nebraska - Lincoln

Anthony F. Starace
University of Nebraska-Lincoln, astarace1@unl.edu

Photodetachment of Na^-

Chien-Nan Liu and Anthony F. Starace
Department of Physics and Astronomy, The University of Nebraska, Lincoln, Nebraska 68588-0111
(Received 13 November 1998)

Eigenchannel *R*-matrix calculation results are presented for the photodetachment partial cross sections of Na^- for energies up to the Na($5p$) threshold. The photoelectron angular distribution asymmetry parameter for the process $Na^- + \gamma \rightarrow Na(3p) + e^-$ is also presented over the same energy range. Detailed analyses and identifications of $^1P^o$ resonance structures are presented and compared with corresponding ones in H^- and Li^-. Our results are compared with works of others, including the four-state close-coupling results of Moores and Norcross [Phys. Rev. A **10**, 1646 (1974)], the resonances observed by Johnston and Burrow [Phys. Rev. A **51**, 406 (1995)] in studies of temporary negative ion formation in electron scattering by Na atoms, and the recent relative Na($4s$) partial cross-section measurements of G. Haeffler *et al.* [following paper, Phys. Rev. A **59**, 3655 (1999)]. [S1050-2947(99)11505-1]

PACS number(s): 32.80.Gc, 31.25.Jf, 31.50.+w

I. INTRODUCTION

Theoretical and experimental studies of photodetachment of negative ions have long been justified on the basis of their importance to low-temperature plasma spectroscopy, upper atmosphere studies, and astrophysics. Recent technological advances, however, have so greatly expanded both theoretical and experimental capabilities that studies of photodetachment of negative ions accompanied by high levels of excitation of the residual atom are now possible. Typically, below each excitation threshold, the structure of the spectrum is dominated by two-electron resonances. In contrast to spectra of neutral atoms, there are no Rydberg series of resonances to obscure the effects of the more interesting correlated, two-electron states. Thus an additional justification for studies of photodetachment plus excitation of negative ions is to determine and understand the effects of highly correlated, two-electron states on these processes.

There are relatively few theoretical or experimental studies of highly excited, two-electron states in photodetachment of negative ion systems other than for H^- and Li^-. H^- is of course the prototype for such studies. Many schemes for the classification of its resonance states have been proposed which reveal the underlying symmetry of these pure, three-body Coulomb states [1–4]. Experimental measurements have been reported by Harris *et al.* [5] and the major structures in these spectra appearing below the excited atomic state thresholds have been interpreted as reflecting propensity rules [6,7] for populating ''+'' type doubly excited states.[1] In addition, some weak features have been identified as due to population of propensity-rule-forbidden states having ''−'' character [8].[2] There have also been many studies involving accurate calculations of the energies and widths of the doubly excited states in H^- [9]. Because of the similarities of its structure to that of H^-, Li^- has been a focus of a number of recent theoretical [10–13] and experimental [14–16] studies. The theoretical studies in Refs. [10,12,13] reveal that the nonhydrogenic core of Li^+ leads to prominence of some propensity-rule-forbidden, doubly excited resonances that are absent in H^- photodetachment spectra.

In contrast to the relatively large number of recent studies of highly excited two-electron states in photodetachment spectra of H^- and Li^-, the Na^- photodetachment spectrum and, more specifically, the spectrum of excited two-electron states in Na^-, is relatively unexplored. There have been a number of theoretical calculations of Na^- photodetachment over the energy region up to the first excited atomic threshold, Na($3p$) [17–22]. While the earliest of these calculations are rather crude [17,18], Moores and Norcross [19] obtained good agreement with the relative experimental measurements of Patterson, Hotop, and Lineberger [23] in the region of the Na($3p$) threshold using a four-state (i.e., $3s$, $3p$, $4s$, and $3d$) close-coupling calculation in which the outer two electrons move in the field of an effective potential representing the nucleus plus inner shell electrons. The semi-empirical model potential results of Stewart, Laughlin, and Victor [20] and the *K*-matrix results of Moccia and Spizzo [22] are in excellent agreement with the Moores and Norcross [19] close-coupling results. The random phase approximation (RPA) results of Amusia *et al.* [21] disagree with the results of Moores and Norcross [19], and, in particular, they fail to describe the cusplike behavior at the Na($3p$) threshold. However, when the polarization of the Na atom by the detached electron is included, then excellent agreement with the results of Moores and Norcross [19] is obtained above the Na($3s$) threshold. Absolute experimental measurements for the Na^- photodetachment cross section using a crossed

[1]More specifically, in the $(K,T)^A$ notation of Refs. [1,2], these states have been identified as having the angular symmetry $(n-2,1)^+$ [6], where n is the principal quantum number of the lower energy electron. Alternatively, in the molecular-type classification scheme of Ref. [3], they are said to correspond to transitions involving a change in the vibrational quantum number of unity, i.e., $\Delta v_2 = +1$ [7].

[2]More specifically, these structures have been identified in Ref. [8] as having the angular symmetry $(K,T)^A = (n-1,0)^-$.

beam technique have been made by Kaiser *et al.* [24], but their results are much lower than the predictions of Moores and Norcross [19] and fail to describe the cusplike behavior near the Na($3p$) threshold that is shown by the experimental results of Patterson *et al.* [23]. Very recently, Haeffler *et al.* [25] have reported experimental measurements of the Na^- partial cross section for the process $Na^- + \gamma \rightarrow Na(4s) + e^-$ for energies from the vicinity of the Na($5s$) threshold to the vicinity of the Na($4d$) threshold.

We present here a detailed theoretical study of photodetachment spectra of Na^-. Both total and partial cross sections are presented. For energies in the vicinity of the $5s$ and $4d$ thresholds, we compare our results with recent experimental measurements of Haeffler *et al.* [25], and for energies up to the Na($3p$) threshold, we compare our results with those of Moores and Norcross [19]. We also present results for the photoelectron angular distribution asymmetry parameter β for the process $Na^- + \gamma \rightarrow Na(3p) + e^-$, which reveals a rich resonance structure that is absent from the results of Moores and Norcross [19]. The main focus of this paper is on the identification and analysis of these two-electron resonance structures that appear in all partial cross sections above the Na($3p$) threshold. We discuss our method for identifying these resonances, which is akin to methods for identifying resonances in H^- spectra, but which takes into account the nondegenerate thresholds in Na. We analyze graphically the angular symmetries of key resonances using probability density plots and identify those that violate propensity rules developed for H^- photodetachment [6,7]. We also point out the mirroring behavior of the various partial cross sections, which we have recently proved to be a common feature of partial cross sections involving high excitations of the residual atom [26]. Finally, we are able to identify many of the unidentified resonances observed in electron-sodium scattering experiments by Johnston and Burrow [27] and also identify many additional ones that have not yet been seen.

II. THEORY

The eigenchannel *R*-matrix method employed here has proved successful in previous applications to H^- and Li^- photodetachment [10,12,13]. Our methods have been described in detail in Ref. [12] and thus we give here only a brief overview of the method. We then focus our attention in the rest of this section on our methods for analyzing excited, two-electron resonances.

A. Brief overview of the eigenchannel *R*-matrix method

The eigenchannel *R*-matrix method [28,29] aims to determine variationally an orthogonal and complete basis set of wave functions, the eigenchannel wave functions, at energy E, whose normal logarithmic derivatives are constant across a reaction surface S enclosing a reaction volume V. For treatments of two-electron excitations, the reaction volume V is that part of six-dimensional configuration space for which both electrons lie within a sphere of radius r_0. The reaction surface S is the set of points for which $\max(r_1, r_2) = r_0$, where r_1 and r_2 are the electron distances from the nucleus. In practice, for each range of excitation energy, r_0 is chosen to be sufficiently large that the probability of both electrons being outside r_0 is negligible. Thus, r_0 has to be large enough to encompass all possible doubly excited state wave functions in the energy range considered. The complicated many-electron interactions within V are treated by bound state, configuration interaction (CI) techniques using a basis of independent electron orbital wave functions obtained from a Na^+ model core potential and LS coupling to represent the many-electron wave function. The model core potential has the form

$$V(r) = -\frac{1}{r}[Z_c + (Z - Z_c)e^{-a_1 r} + a_2 r e^{-a_3 r}] - \frac{\alpha_c}{2r^4}(1 - e^{-(r/r_c)^3})^2. \quad (1)$$

For our Na^- calculation, the nuclear charge is $Z = 11$, and the charge of the Na^+ core is $Z_c = 1$. The polarizability of the Na^+ core is taken to be $\alpha_c = 0.9457$ a.u. [30]. The empirical parameters (a_1, a_2, a_3, r_c) are fitted using a least-squares method to reproduce the experimentally measured energy levels of the Na atom [31] and have the values $a_1 = 3.324\,424\,5$, $a_2 = 0.713\,727\,9$, $a_3 = 1.832\,818\,2$, and $r_c = 0.524\,506\,3$. At a given energy E, one describes the wave function inside the reaction volume as a linear combination of eigenchannel wave functions thus generated. Outside r_0 it is assumed there is only a single electron, and thus only single detachment processes are considered. All long-range multipole interactions in the outer region are treated numerically by close-coupling procedures in order to obtain a base set of multichannel wave functions which describe the outgoing electron and the atomic core. By thus treating the long-range multipole interactions, we are able to use much smaller values of r_0 than would otherwise be the case. By matching linear combinations of the multichannel base functions for the inner and outer regions at the reaction surface, one can determine the exact wave function which satisfies the incoming wave boundary condition. Further details of our methods are presented in Ref. [12].

B. Identification of doubly excited states

In order to analyze the resonances in the photodetachment spectra, we use a Feshbach projection operator technique to obtain the wave functions for the doubly excited states that are responsible for them. According to the standard method, doubly excited states associated with the nl threshold are obtained by diagonalizing the Hamiltonian using a basis that excludes all one-electron orbitals lower in energy than nl, since such orbitals serve to represent open channels. In other words, this is a CI calculation within a subset of the configuration space. One seeks to obtain eigenstates below the nl threshold, which would correspond to autodetachment resonances associated with the threshold. To test whether a wave function of a doubly excited state thus generated truly represents the resonance feature appearing in our full calculation, we project out the doubly excited wave function from our full final state wave function, and check whether the resonance feature in the cross section is removed. However, the degree to which electron correlation effects are faithfully de-

scribed is very sensitive to the theoretical approach employed to calculate the doubly excited state wave function. Due to the nondegeneracy of the atomic thresholds of Na and the strong spatial overlap of orbitals belonging to adjacent thresholds, a doubly excited resonance series converging to a given threshold often overlaps spatially with the orbitals of the lower threshold. We have found that the standard projection operator method does not explain the resonance structure very well when such overlap with lower threshold orbitals is significant. So, instead of considering each nl threshold separately, we consider adjacent thresholds together and make the following modifications to the standard procedure. We apply the standard projection operator method with respect to the threshold of higher energy to construct the Hamiltonian, but include also some additional configurations having the orbital of the lower energy threshold in order to describe any doubly excited states that are associated with the lower threshold. Such states are generally referred to as core-excited shape resonances. For example, in diagonalizing the Hamiltonian to find doubly excited states in the neighborhood of the Na($5s$) and Na($4d$) thresholds, we exclude all configurations having orbitals below $4d$ with the exception of the two configurations $5s5p$ and $5s6p$. We find such a nonstandard method gives a better description of the doubly excited resonances. In particular, despite the inclusion of a few configurations having orbitals associated with the lower threshold, the resonance states that we calculate are in general more localized than are those obtained using the standard procedure.

To demonstrate the effect of removing each doubly excited state, we show the cross sections obtained by orthogonalizing our final state wave functions to them. Thus, we can correlate the wave-function properties of these states and the resonance features in the spectra, shedding light on the propensity rules in photodetachment processes of two-electron systems. This procedure also provides a useful check of a particular doubly excited state wave function obtained by the nonstandard projection operator method in that one can see the extent to which it is responsible for the corresponding resonance feature in the spectrum.

The identification of doubly excited states is made by a comparison of their probability density distributions with those of the corresponding states in the pure three-body Coulomb system, H^-. In comparing the probability density distributions, we examine primarily the pattern of their nodes and antinodes. In order to facilitate the designation in different notations, all plots are made in three different ways: in (r_1,r_2) coordinates; in hyperspherical angle coordinates (α, θ_{12}); and in prolate spheroidal coordinates (μ,λ). However, both group notation, e.g., $(K,T)^A$, and molecular-orbital notation, (n_λ,n_μ,m), are more approximate designations when applied to alkali-metal negative ion, doubly excited states owing to the non-Coulomb core.

C. Numerical aspects

We present here some of the numerical details of our calculations. The radius of the R-matrix sphere, r_0, is chosen to be 180 a.u. The probability density plots of the doubly excited states indicate that it is big enough to encompass the doubly excited states in the energy range considered. Inside the R-matrix sphere, 58 closed-type (i.e., zero at the radius r_0) and two open-type (i.e., nonzero at the radius r_0) one-electron orbital wave functions are calculated for each of the orbital angular momenta $0 \leqslant l \leqslant 6$. In total, we include 2507 closed-type, two-electron configurations in the calculation for the final state wave function. For each channel in which one electron can escape from the reaction volume, we include two open-type orbitals for the outer electron in addition to the closed-type basis set. For a given photon energy, besides all open channels, closed channels having the inner electron at the next higher principal quantum number state are also included in the calculation.

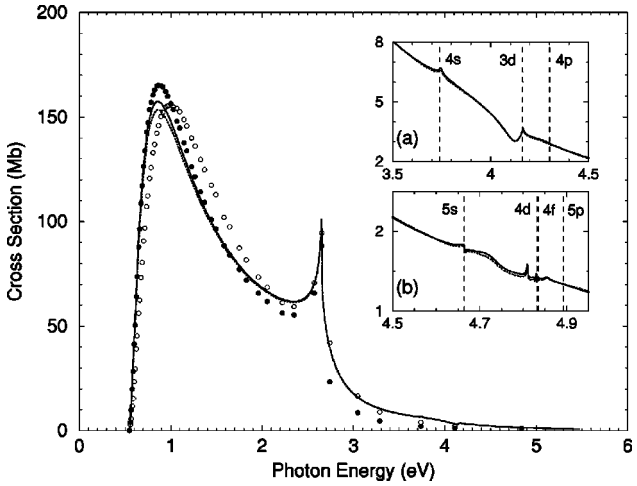

FIG. 1. Total cross section for photodetachment of Na^- vs photon energy. Present dipole length (velocity) results are plotted using dotted (solid) lines. Open (filled) circles indicate the dipole length (velocity) results of Moores and Norcross [19]. Insets show the regions near excited state thresholds, Na(nl), whose positions are indicated by the vertical dashed lines.

III. RESULTS

A. Overview of the region from the detachment threshold to the Na($6p$) excitation threshold

In Figs. 1 and 2, we present an overview of our results of photodetachment of Na^-. Figure 1 shows the present results for the total cross section together with the four-state close-coupling calculation results of Moores and Norcross [19]. The energy range encompasses the region from the threshold of the Na ground state to just above the Na($6p$) excitation threshold. The inset figures examine regions where weaker but richer resonance structures near higher thresholds are found in the present calculations. Detailed analyses of these energy regions are given in the following sections. While the results of Moores and Norcross [19] agree with the present results in the region below the first excited threshold, their simple model fails to account for the resonance structures at higher thresholds.

The Na^- spectrum, like that of Li^-, is dominated by its features below the first excited state threshold. Namely, the photodetachment cross section rises rapidly above the ground-state threshold and exhibits a prominent cusp structure at the first excited state threshold, Na($3p$). The cusp behavior is well understood on the basis of Wigner threshold laws [32]. However, a number of authors have investigated

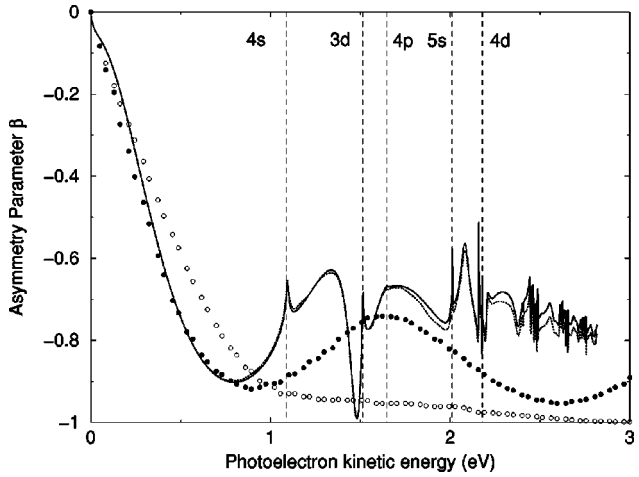

FIG. 2. Angular distribution asymmetry parameter β of the photoelectron resulting from the process $Na^- + \gamma \rightarrow Na(3p) + e^-$, plotted vs photoelectron kinetic energy. Present dipole length (velocity) results are shown using dotted (solid) lines. Open (filled) circles indicate the dipole length (velocity) results of Moores and Norcross [19]. The dashed lines indicate the locations of the Na(nl) thresholds.

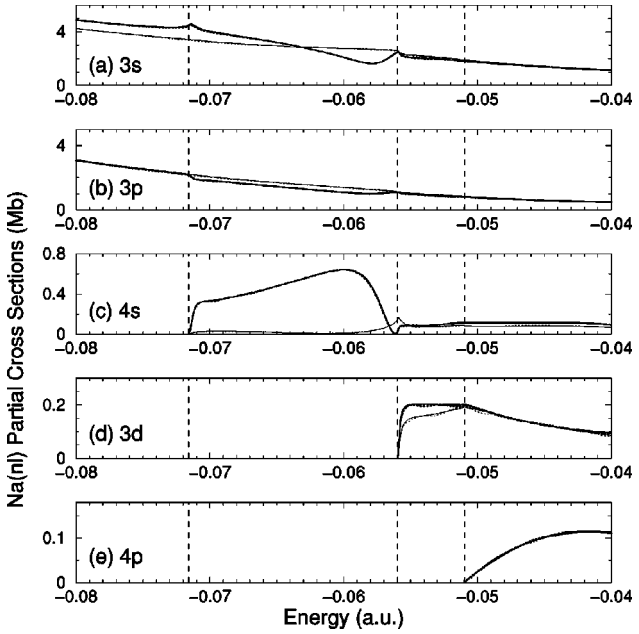

FIG. 3. Partial cross sections for the process $Na^- + \gamma \rightarrow Na(nl) + e^-$, for $nl = 3s$, $3p$, $4s$, $3d$, and $4p$. The energy scale is relative to the Na^+ threshold. Thick curves: present results in dipole velocity (solid) and dipole length (dotted) gauges. Thin curves: results obtained by removing the doubly excited state located at $-0.061\,46$ a.u. ($\hbar\omega = 4.0145$ eV) from the calculations. This doubly excited state is obtained by our nonstandard projection operator method. Vertical dashed lines indicate the locations of the Na(nl) thresholds.

whether or not there is also a resonance associated with the cusp feature. Moores and Norcross [19] argue that their calculations at the Na($3p$) threshold show the Wigner threshold law to be valid over only a very narrow energy range. Since the cusp structure in their calculation extends over a broader energy range, they make the assumption that a near-threshold resonance must be affecting the calculated results. Moccia and Spizzo [22], however, note that ''this [cusp] structure is best ascribed to threshold effects rather than to a resonance.'' The cusp behavior has been observed in both the photodetachment experiment of Patterson *et al.* [23] and the electron-sodium collision experiments of Eyb and Hofmann [33]. Johnston and Burrow also observe a strong feature near the Na($3p$) threshold in electron-transmission spectroscopy [27]. However, except for one CI calculation that predicts the existence of a $^1P^o$ Feshbach resonance below the Na($3p$) threshold [34], there is no definite experimental observation or theoretical prediction of any $^1P^o$ resonance near the Na($3p$) threshold. In contrast, photodetachment experiments for Rb^- and Cs^- reveal definite narrow windows below the first excited ^2P threshold [35], confirming the existence of $^1P^o$ resonances in these heavier negative alkali-metal ions. Moores and Norcross find that the photoelectron phase shift in Na^- photodetachment exhibits a sharp increase, but fails to reach $\pi/2$ before the Na($3p$) threshold [19], indicating the intervention of the channel opening before the resonance is fully developed [35]. Some theoretical calculations for electron-sodium collisions also predict a similar phase shift increase in the ^1P channel near the 3p threshold [36,37], but no definite resonance energy has been given. In our own calculations we find no evidence of the existence of any Feshbach resonance state.

Our results for the angular distribution asymmetry parameter β of the photoelectron resulting from the process $Na^- + \gamma \rightarrow Na(3p) + e^-$ are presented in Fig. 2 together with those of Moores and Norcross [19]. The resonance structures are observed to be more complex since β parameters are ratios of transition matrix elements for different channels. Our results agree well with those of Ref. [19] from the Na($3p$) threshold up to 0.3 eV, but our length and velocity results are in much closer agreement. The complex resonance structure we predict in the energy region above 0.8 eV is not described at all by the four-state close-coupling results of Ref. [19].

B. Na^- photodetachment near the Na4*s* and 4*p* thresholds

Partial cross sections for all open channels in the energy range from below the Na($4s$) threshold to above the Na($4p$) threshold are shown in Fig. 3. Below the Na($3d$) threshold, the cross section is apparently dominated by a broad doubly excited state resonance. There are two major features associated with this resonance. First, it is so broad that it overlaps the Na($4s$) threshold. Second, this resonance is particularly prominent in the $4s$ partial cross section. In order to account for these and any other resonance features, the nonstandard projection operator method was used to search for doubly excited states. All configurations having orbitals lower in energy than $3d$ are excluded in the Hamiltonian except for the configuration $4s4p$. Only one doubly excited state at $-0.061\,46$ a.u. (or at a photon energy of 4.014 eV) is found below the Na($3d$) threshold. We also show in Fig. 3 the cross sections that result after removing this specific doubly excited state, thus verifying that it alone accounts for the resonance features predicted in this energy region. Our attribution of all resonance effects to this single doubly excited state contradicts the CI calculation of Zatsarinny *et al.* [34], which predicts three $^1P^o$ autoionizing states at photon ener-

gies of 4.10, 4.12, and 4.16 eV (or at total energies of -0.059, -0.058, and -0.056 a.u.). Stewart *et al.* also predict a $^1P^o$ resonance at -0.0567 a.u. (or $\hbar\omega = 4.122$ eV) using the standard projection operator method [20]. The discrepancies among these various theoretical predictions arise because the two calculations [20,34] other than our own are not able to predict core-excited shape resonances owing to their neglect of the $4s4p$ configuration.

Johnston and Burrow observe a resonance feature at about the same energy in electron-transmission spectroscopy [27]. In order to characterize this feature, they related it to a similar-looking resonance appearing below the $K(3d)$ threshold in electron-potassium scattering measurements by Eyb [38], who observed an angular distribution characteristic of a d wave. They suggest a term designation of ^3D owing to an analysis of the results of Eyb, and further suggest a configuration of $4s3d$ for this resonance, noting that ''this configuration is consistent with our unpublished trapped-electron measurements in which the resonance in Na appears rather strongly in the 4^2S excitation cross section [27].'' In accord with our analysis, they note the significant contribution of the $4s$ orbital to the resonance between the Na($4s$) and Na($3d$) thresholds. While our photodetachment results are not able to give any information on the ^3D resonance spectrum, the fact that Johnston and Burrow see only one resonance at about the same energy as our $^1P^o$ resonance may indicate that the $^1P^o$ resonance is too weak to be observed in electron scattering or that it overlaps with the ^3D resonance. In either case, their analysis finds a significant $4s$ contribution to the resonance(s) in this energy region, which is in agreement with our analysis.

The single doubly excited state that we predict is responsible for nearly all of the structure in the partial cross sections shown in Fig. 3 is dominated by the $4s4p$ (36.2%) and $3d4p$ (34.4%) configurations. Its position is well above the Na($4s$) threshold; thus it has mixed characteristics of both a core-excited shape resonance and a Feshbach resonance. Its configuration components are similar to the resonance appearing between the Li($3s$) and Li($3p$) threshold, which is dominated by the $3s3p$ (35.2%) and $3p3d$ (34.1%) configurations. Actually, wave functions of these two states, one each in the photodetachment spectra of Li^- and Na^-, display the same angular symmetry as the one denoted by ${}_3\{0\}_3^+$ [equivalent to $(K,T)^A=(1,1)^+$ or $(n_\lambda,n_\mu,m)=(0,2,1)$] in H^- photodetachment below the $n=3$ threshold. A comparison of this resonance in H^- with the corresponding one in Na^- is shown by the density plots in Fig. 4. Notice the additional peak near α equal to 0 (or $\pi/2$) in the hyperspherical angular plot for Na^- [cf. Fig. 4(a)], which indicates an additional node and hence a $4s$ orbital contribution, as the Na($4s$) threshold lies below both the Na($3d$) threshold and the resonance energy. Such peaks are absent in the density plot for the corresponding state in H^- [cf. Fig. 4(b)]. The important $4s$ orbital contribution explains the breadth of this resonance, as well as its prominence in the $4s$ partial cross section. The importance of the $nsnp$ component of the resonance above the ns threshold indicates the complexity of the correlation. In the standard projection operator method, this configuration would be excluded.

The effectiveness of our nonstandard projection operator method for describing this resonance may be judged by comparing our results with those obtained using the standard projection operator method. The standard method finds a resonance at $\hbar\omega = 4.1432$ eV (or $-0.056\,73$ a.u. below the Na^+ threshold). Its density plots are shown in Fig. 4(c). Comparing Figs. 4(a) and 4(c), one sees the standard method gives a much more diffuse state having a different angular symmetry. The results of the Na($3s$), Na($3p$), and Na($4s$) partial cross sections after projecting out the doubly excited state obtained by the standard method are given in Fig. 5. Comparing Figs. 3(c) and 5(c), we see that our nonstandard method produces a localized resonance which is responsible for essentially all the magnitude of the Na($4s$) partial cross section between the Na($4s$) and Na($3d$) thresholds. In contrast, the standard method gives a resonance whose major effect is near the Na($3d$) threshold.

Figure 6 shows the β parameter for the photoelectron resulting from the process $Na^- + \gamma \rightarrow Na(3p) + e^-$. Besides the two cusp features associated with the Na($4s$) and Na($3d$) thresholds, there is a complex resonance structure between these two thresholds. It is interesting that the β parameter approaches -1 below the Na($3d$) threshold, implying that the preferred angular distribution of the photoelectron there is at 90° to the laser linear polarization direction. In Fig. 6, the light lines indicate results obtained by removing the effects of the ${}_3\{0\}_3^+$ resonance at 1.3628 eV photoelectron kinetic energy. One sees that this resonance is responsible for both the broad peak and the deep window that appear in our results below the Na($3d$) threshold.

Between the Na($3d$) and Na($4p$) thresholds, our analysis using the standard projection operator method also finds a ''$-$'' type resonance state located at $-0.051\,10$ a.u. (or $\hbar\omega = 4.2966$), in agreement with the results Zatsarinny *et al.* [34]. However, the effects of this resonance state are not so prominent and hence are not analyzed in either Fig. 3 or Fig. 6 although, of course, these effects are included in our results.

C. Na^- photodetachment near the Na $5s$, $4d$, $4f$, and $5p$ thresholds

Partial cross sections for all open channels in the energy range from below the Na($5s$) threshold to just above the Na($5p$) threshold are shown in Fig. 7. Compared with the energy region near lower thresholds, the partial cross sections show more complex resonance structures. While no $^1P^o$ resonance has been predicted in the energy region between the Na($5s$) and Na($4d$) threshold, our nonstandard projection operator method analysis indicates there are five doubly excited state resonances in this energy region. As shown in Fig. 8, our Na($4s$) partial cross-section results give excellent predictions of the positions and widths of the resonances as well as with the broad shape of the spectrum as compared with recent relative measurements of Haeffler *et al.* between the Na($5s$) and Na($5p$) thresholds [25]. However, some discrepancies in the magnitudes may be observed for photon energies above 4.75 eV, particularly above the Na($4d$) threshold. We have confirmed the convergence of our results in this region and have no theoretical explanation for these discrepancies. However, as shown in the inset fig-

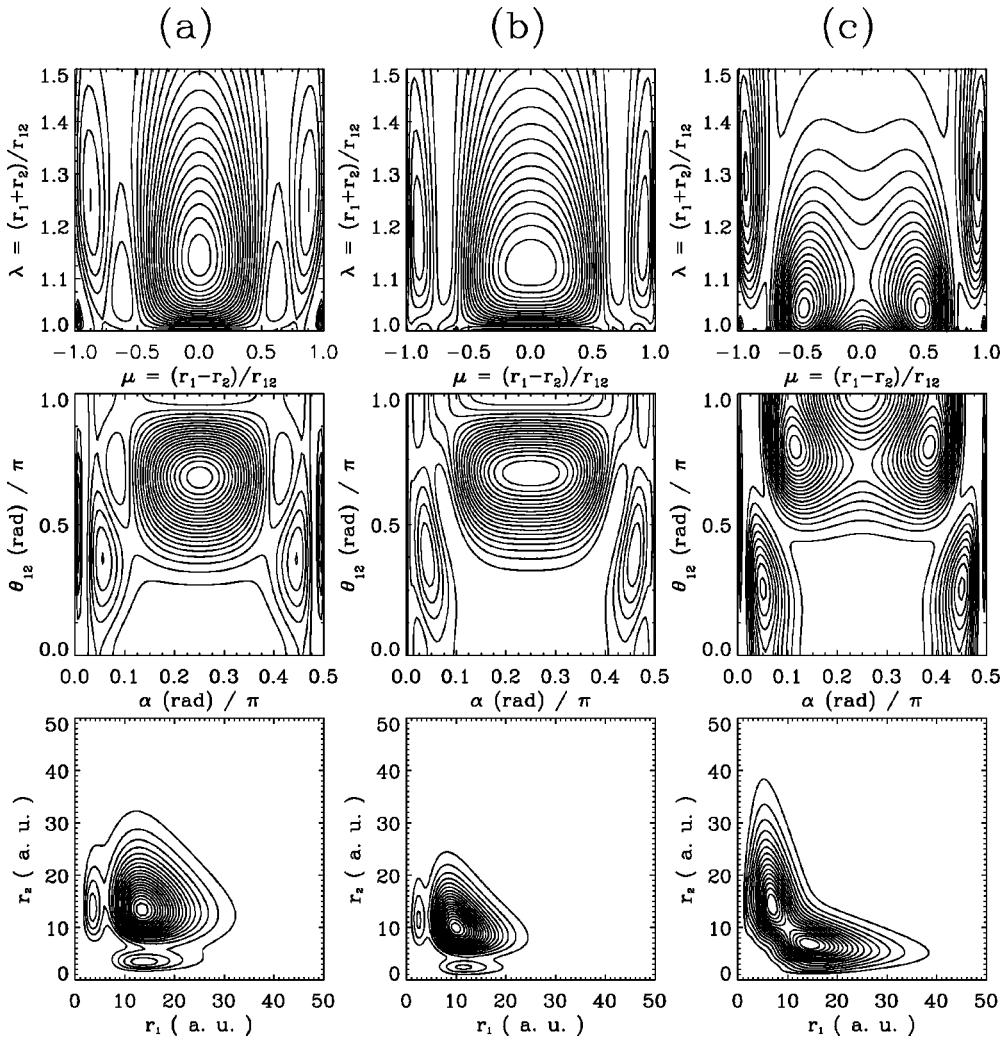

FIG. 4. Doubly excited state $(K,T)^A=(1,1)^+$ wave-function density plots in (a) Na^- and (b) H^-. This state in Na^- is located at $-0.061\,46$ a.u. ($\hbar\omega=4.0145$ eV); it is obtained using our nonstandard projection operator method and its effects on the partial cross sections are shown in Fig. 3. In (c) we give the doubly excited state wave-function density plots for Na^- for the state located at $-0.056\,73$ a.u. ($\hbar\omega=4.1432$); it is obtained using the standard projection operator method and its effects on the partial cross sections are shown in Fig. 5. The top panels are plotted in prolate spheroidal coordinates λ and μ at a value of $R=\sqrt{r_1^2+r_2^2}$ which corresponds to the maximum wave-function amplitude; the middle panels are plotted in hyperspherical coordinates θ_{12} and $\alpha\equiv\tan^{-1}(r_2/r_1)$ at the same value of R; the bottom panels are plotted in (r_1,r_2) coordinates with angular variables averaged.

ure, when the experimental data between the Na($4d$) and Na($5p$) thresholds are normalized to our theoretical predictions in this energy region, the agreement is excellent. As noted in Ref. [25], this may indicate a problem with the background above the Na($4d$) threshold.

Some observations can be made regarding these total and partial cross sections shown in Fig. 7. The Na($3s$) and Na($3p$) partial cross sections give the largest contribution to the total cross section; the other partial cross sections are relatively small. Since most of the doubly excited states involve orbitals associated with higher thresholds, the effect of these resonance states is largest on the partial cross sections having the smallest magnitude. Indeed, these partial cross sections are often completely dominated by the doubly excited resonances, showing such interference effects as asymmetric peaks and nearly zero minima. However, these resonance features are not prominent in the total cross section, indicating that only a relatively small fraction of the total cross section interacts with these doubly excited states, i.e., the correlation index, ρ^2, of Fano and Cooper [39] is small. Liu and Starace [26] have recently proved that when $\rho\to 0$, mirroring behavior of partial cross sections is to be expected. We point out here such behavior in the partial cross sections shown in Fig. 7, e.g., the Na($4p$) and Na($5s$) partial cross sections between the $5s$ and $4d$ thresholds are nearly mirror images of one another.

In the energy region shown in Fig. 8 we find that five doubly excited states are responsible for the structure in the spectrum. The effects of each of these five resonances on the Na($4s$) partial cross section shown in Fig. 8 are shown in panels (a)–(e) of Fig. 9. Panel (f) in Fig. 9 shows the effect of removing all five resonances. The nearly linear cross section that results [cf. Fig. 9(f)] proves that the five resonances we have identified are indeed responsible for all the observed structure. Figure 10 gives a similar analysis of the effect of each of these five resonances on the photoelectron angular distribution asymmetry parameter β for the process $Na^- + \gamma\to Na(3p)+e^-$ in this energy region. Figure 10(f) shows

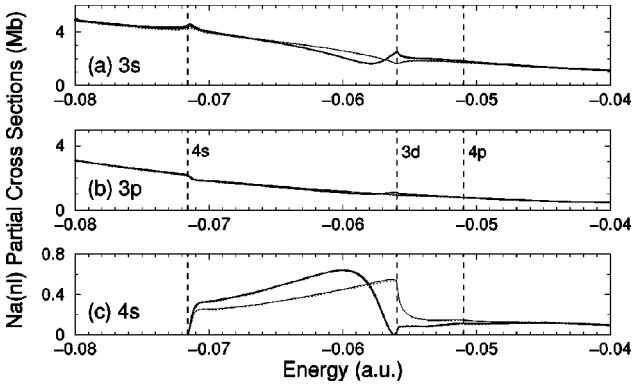

FIG. 5. Partial cross sections for the process $Na^- + \gamma \rightarrow Na(nl) + e^-$, for $nl = 3s$, $3p$, and $4s$. The energy scale is relative to the Na^+ threshold. Thick curves: present results in dipole velocity (solid) and dipole length (dotted) gauges. Thin curves: results obtained by removing the doubly excited state located at $-0.056\,73$ a.u. ($\hbar\omega = 4.1432$ eV) from the calculations. This doubly excited state is obtained by the standard projection operator method. Vertical dashed lines indicate the locations of Na(nl) thresholds.

that removing each of these five resonances results in a smooth linear dependence for the β parameter, proving again that they are solely responsible for the observed structure in the β parameter. Density plots for each of these five resonances are presented in Fig. 11, plotted in both prolate spheroidal coordinates and hyperspherical angle coordinates at the values of $R \equiv \sqrt{r_1^2 + r_2^2}$ indicated in the figure caption. The densities are also plotted in angle-averaged (r_1, r_2) coordinates. We discuss the characters of each of these five resonances in turn.

There is a broad ''+'' type resonance state located below the Na($5s$) threshold at a photon energy of 4.6557 eV (or

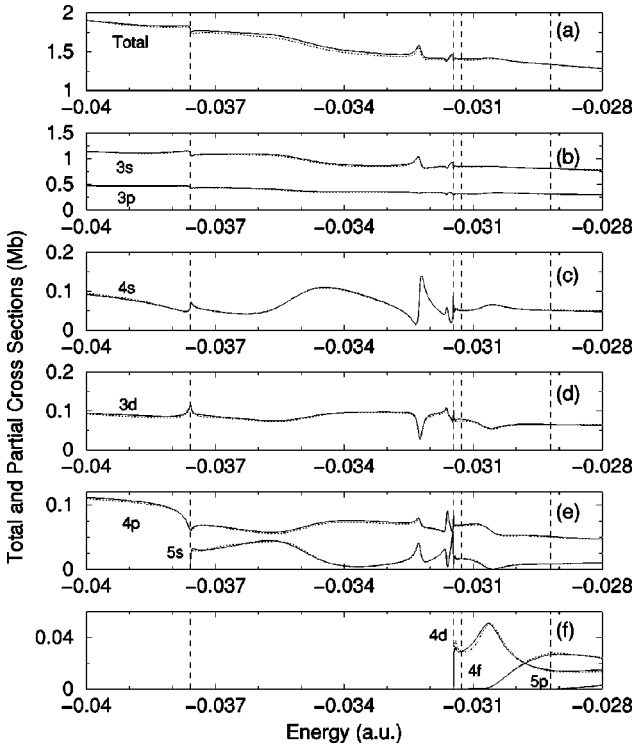

FIG. 7. Partial cross sections for the processes $Na^- + \gamma \rightarrow Na(nl) + e^-$, $nl = 3s$, $3p$, $4s$, $3d$, $4p$, $5s$, $4d$, $4f$, and $5p$, and the total cross section. The energy scale is relative to the Na^+ threshold. The vertical dashed lines indicate the locations of the thresholds.

$-0.037\,90$ a.u. below the Na^+ threshold) [cf. Figs. 8, 9(a), and 10(a)]. Its most important configurations are $5s5p$ (35.56%), $5s6p$ (27.26%), and $4d5p$ (20.67%). Its probability density angular plots in Fig. 11(a) show a mixture of the

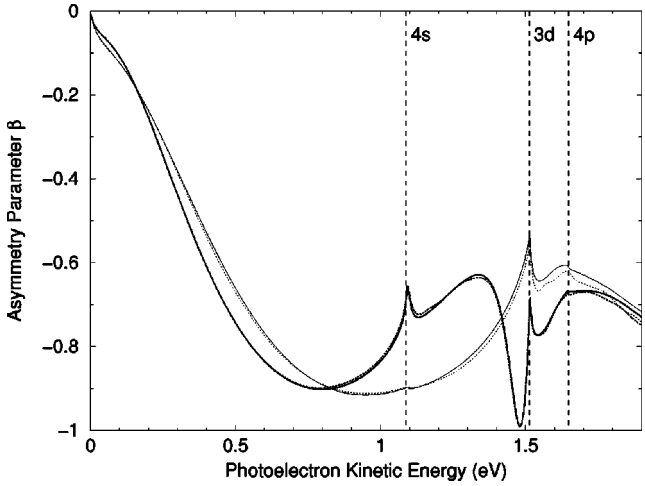

FIG. 6. Angular distribution asymmetry parameter β of the photoelectron resulting from the process $Na^- + \gamma \rightarrow Na(3p) + e^-$, plotted vs photoelectron kinetic energy. The plot shows the energy region from the Na($3p$) threshold to above the Na($4p$) threshold. Thick curves: present results in dipole velocity (solid) and dipole length (dotted) gauges. Thin curves: results obtained by removing the doubly excited state located at $-0.061\,46$ a.u. (photoelectron kinetic energy = 1.3628 eV) from the calculation. The vertical dashed lines indicate the locations of the thresholds.

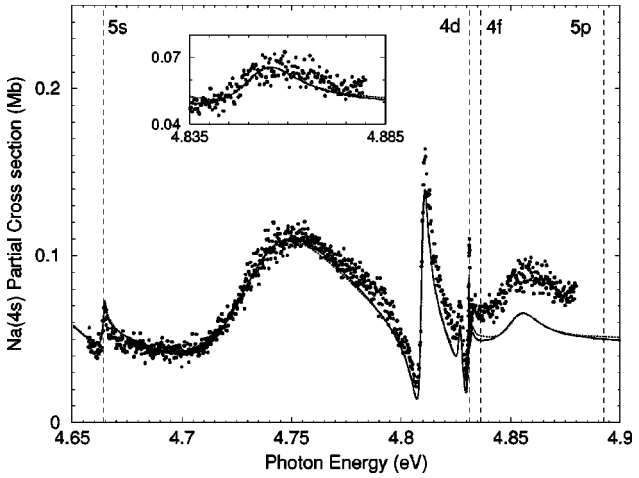

FIG. 8. Partial cross section for the process $Na^- + \gamma \rightarrow Na(4s) + e^-$ in the photon energy region from the Na($5s$) to the Na($5p$) threshold. Curves: present results in dipole velocity (solid) and dipole length (dotted) gauges. Circles: relative experimental measurements of Haeffler *et al.* [25] normalized to the theoretical predictions between the Na($5s$) and Na($4d$) thresholds. The vertical dashed lines indicate the locations of the thresholds. The inset shows a renormalized comparison between theory and experiment between the Na($4d$) and Na($5p$) thresholds.

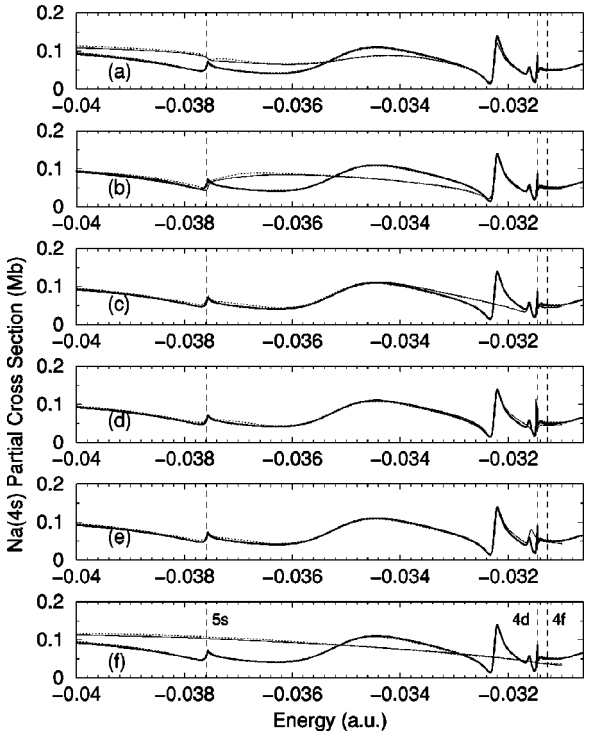

FIG. 9. Partial cross section for the process $Na^- + \gamma \rightarrow Na(4s) + e^-$ in the energy range from below the Na($5s$) threshold to above the Na($4f$) threshold. The energy scale is relative to the Na^+ threshold. Thick curves: present results in dipole velocity (solid) and dipole length (dotted) gauges. Thin curves: results obtained by removing one or more doubly excited states from the calculations. (a) Doubly excited state with symmetry $(K,T)^A=(2,1)^+$ at $-0.037\,90$ a.u. ($\hbar\omega=4.6557$ eV) removed; (b) doubly excited state with symmetry $(K,T)^A=(3,0)^-$ at $-0.034\,93$ a.u. ($\hbar\omega=4.7365$ eV) removed; (c) doubly excited state with symmetry $(K,T)^A=(2,1)^+$ at $-0.032\,29$ a.u. ($\hbar\omega=4.8084$ eV) removed; (d) doubly excited state with symmetry $(K,T)^A=(1,0)^-$ at $-0.031\,70$ a.u. ($\hbar\omega=4.8243$ eV) removed; (e) doubly excited state with symmetry $(K,T)^A=(2,1)^+$ at $-0.031\,30$ a.u. ($\hbar\omega=4.8353$ eV) removed; (f) all five doubly excited states removed. The vertical dashed lines indicate the locations of the thresholds.

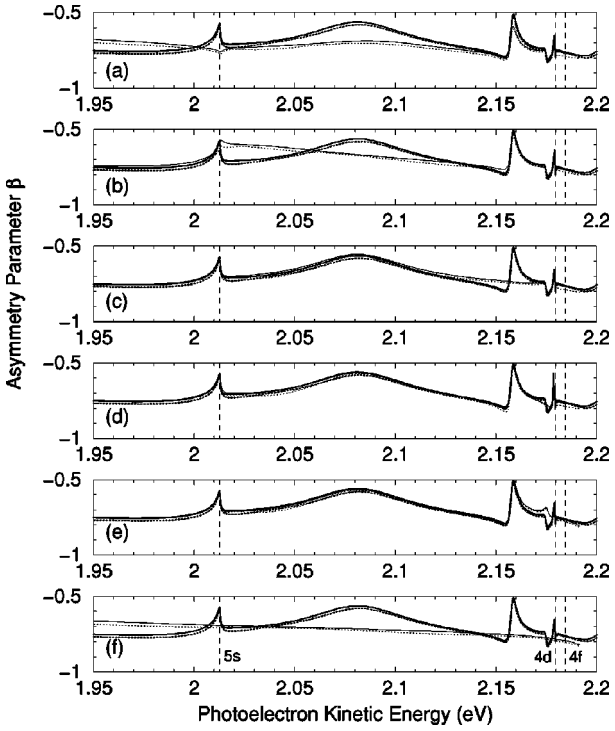

FIG. 10. Angular distribution asymmetry parameter β of the photoelectron for the process $Na^- + \gamma \rightarrow Na(3p) + e^-$, plotted vs photoelectron kinetic energy over the energy region from below the Na($5s$) threshold to above the Na($4f$) threshold. Thick curves: present results in dipole velocity (solid) and dipole length (dotted) gauges. Thin curves: results obtained by removing one or more doubly excited states from the calculations. The specifications of the resonances removed in panels (a)–(f) are the same as in the corresponding panels of Fig. 9.

symmetries of $(K,T)^A=(2,1)^+$ [or $(n_\lambda,n_\mu,m)=(0,4,1)$] and $(K,T)^A=(3,1)^+$ [or $(n_\lambda,n_\mu,m)=(0,6,1)$], which characterize, respectively, the dominant resonances below the $n=4$ and $n=5$ thresholds in H^-. This mixing is indicated by the additional peaks near α equal to 0 (or $\pi/2$) in the hyperspherical angular plot [cf. Fig. 11(a)] and is due to the fact that the Na($5s$) threshold is lower in energy than the Na($4d$) threshold.

The broad feature near photon energy of 4.75 eV in Figs. 8, 9(b), and 10(b) is caused by a ''$-$'' type doubly excited state which is located at a photon energy of 4.736 eV (or $-0.034\,93$ a.u. below the Na^+ threshold). The breadth of this resonance might be explained by the significant contribution made by the $5s6p$ configuration (22.5%). Since the energy position of this resonance is well above the Na($5s$) threshold, this is another example of a core-excited resonance. Compared with wave functions for the doubly excited states of H^-, this state is dominated by the symmetry $(K,T)^A=(3,0)^-$, or $(n_\lambda,n_\mu,m)=(0,7,0)$ [cf. Fig. 11(b)]. Similar to the resonance below the Na($3d$) threshold, the wave-function density plot in hyperspherical angles (or in prolate spheroidal coordinates) shows a weak peak near α equal to 0 or $\pi/2$ (or near $\mu=\pm1$), indicating the presence of the $5s6p$ configuration.

The resonance located at a photon energy of 4.81 eV in Figs. 8, 9(c), and 10(c) is caused by a ''+'' state which is located at a photon energy of 4.8084 eV (or $-0.032\,29$ a.u. below the Na^+ threshold). Its wave-function density plots, shown in Fig. 11(c), indicate this is a $(K,T)^A=(2,1)^+$ or $(n_\lambda,n_\mu,m)=(0,4,1)$ state, which has the same angular nodal structure as the one below the Na($5s$) threshold [cf. Fig. 11(a)]. Its (r_1,r_2) plot shows one node in each direction of r_1 and r_2, implying that it is an excited state of the series of states characterized by $(K,T)^A=(2,1)^+$. However, the nodal lines in its wave-function density plots are not so sharp as in the corresponding ones for doubly excited resonances in H^-, indicating significant mixing of different angular symmetries due to the nonhydrogenic core of Na^+. Similar non-Coulomb core effects on two-electron resonance states have been shown in the analyses of Pan *et al.* [10,12] for the photodetachment spectrum of Li^-.

A ''$-$'' state located at a photon energy of 4.8243 eV (or $-0.031\,70$ a.u. below the Na^+ threshold) is responsible for the peak near 4.825 eV shown in Figs. 8, 9(d), and 10(d). This state is particularly interesting because its correlation pattern, shown in Fig. 11(d), is similar to the one denoted by $(K,T)^A=(1,0)^-$ in H^-, whose probability density has a

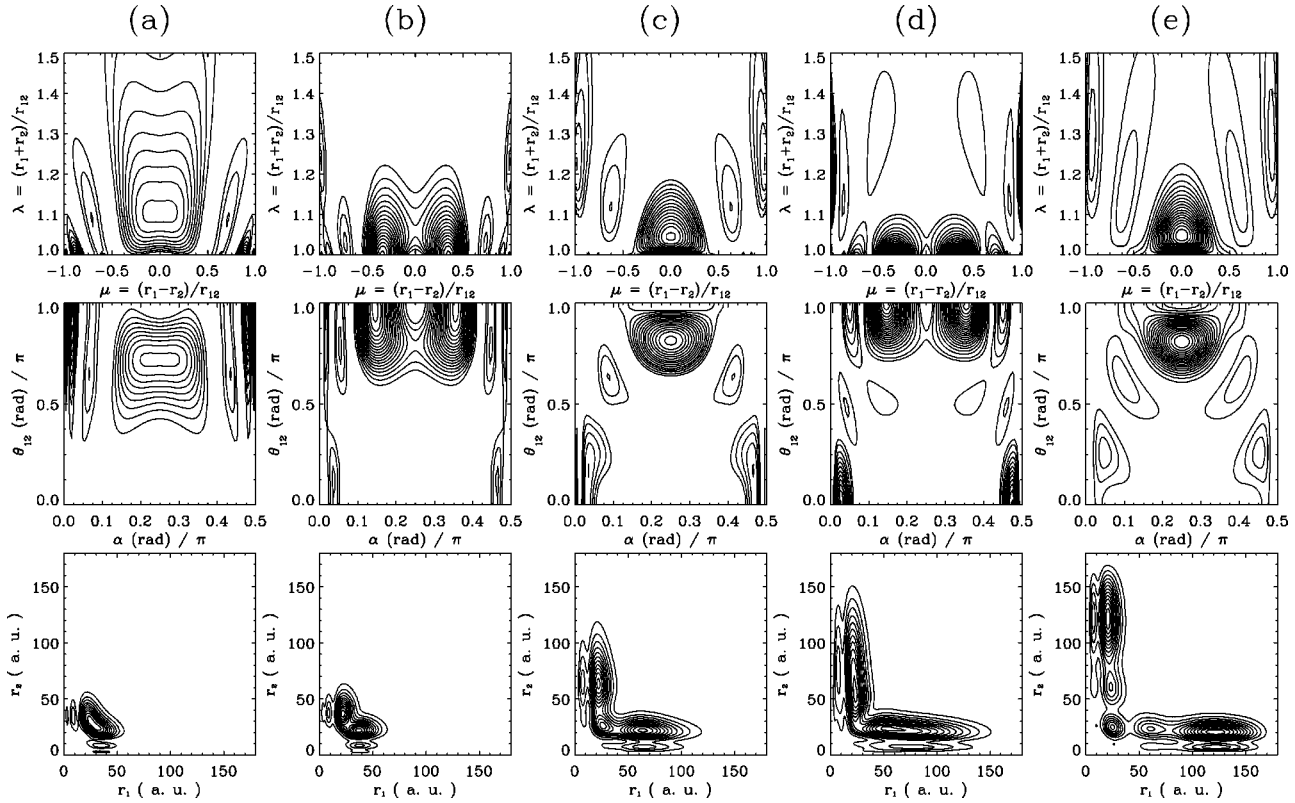

FIG. 11. Wave-function density plots of the doubly excited states below the Na($4d$) threshold. (a) $(2,1)^+$ state at $-0.037\,90$ a.u. ($\hbar\omega=4.6557$ eV) (b) $(3,0)^-$ state at $-0.034\,93$ a.u. ($\hbar\omega=4.7365$ eV), (c) $(2,1)^+$ state at $-0.032\,29$ a.u. ($\hbar\omega=4.8084$ eV), (d) $(1,0)^-$ state at $-0.031\,70$ a.u. ($\hbar\omega=4.8243$ eV), (e) $(2,1)^+$ state at $-0.031\,30$ a.u. ($\hbar\omega=4.8353$ eV). The top panel for each resonance is plotted in prolate spheroidal coordinates at $R=\sqrt{r_1^2+r_2^2}=$ (a) 41 a.u., (b) 43 a.u., (c) 30 a.u., (d) 50 a.u., (e) 30 a.u. The middle panels are plotted in hyperspherical angle coordinates α and θ_{12} at the same R values. The bottom panels are plotted in (r_1,r_2) coordinates with averaging over the angular variables.

nodal line in θ_{12} (equivalently, in λ). This state does not fall in the category of either $(K,T)^A=(n-2,1)^+$ or $(K,T)^A=(n-1,0)^-$ for $n=4$. It is a propensity rule forbidden state and is not seen in the spectra of either theoretical predictions or experimental measurements for H^- photodetachment, but is visible in Na^- photodetachment owing to the non-Coulomb core of Na^+ and the consequent more approximate doubly excited state symmetries.

The window and very narrow peak just below the Na($4d$) threshold in Figs. 8, 9(e), and 10(e) is produced by a ''+'' type state. It can be identified as another $(K,T)^A=(2,1)^+$ state. Compared with the ones at photon energies of 4.6557 eV and 4.8084 eV [cf. Figs. 11(a) and 11(c)], which have, respectively, zero and one node in r_1 and r_2, the wave-function density plot in (r_1,r_2) coordinates [cf. Fig. 11(e)] has two nodes in both r_1 and r_2. Thus it is the third member of the series characterized by $(K,T)^A=(2,1)^+$.

The peak above the Na($4f$) threshold shown in Figs. 7 and 8 at a photon energy of 4.86 eV is actually a doubly excited state associated with the next threshold, Na($5p$), which is located at photon energy of 4.892 eV. The resonance energy from the standard projection operator method is 4.8800 eV (or $-0.029\,66$ a.u. below the Na^+ threshold), which agrees with the result of Zatsarinny *et al.* [34]. This resonance is well resolved both experimentally [25] and theoretically and, as shown in the inset in Fig. 8, agreement is excellent. However, no resonance was reported in electron-transmission spectroscopy experiments [27]. Although it has been suggested [27] that the lack of resonances is due to the negative polarizabilities associated with these excited Na(np) states for $n\geqslant 4$ [40], the existence of a resonance below the Na($5p$) threshold sheds some light on the properties of doubly excited resonances. Negative polarizabilities imply an asymptotically repulsive potential, but at short range the effective electron-electron interaction may be attractive, allowing the existence of a bound state. However, the long-range repulsive potential might be the reason why there is only one doubly excited resonance below the Na($5p$) threshold. Our theoretical prediction employs the standard projection operator method. Owing to the closeness of the resonance to the Na($4d$) and Na($4f$) thresholds, however, we have also carried out a number of nonstandard projection operator calculations that include the configurations $4d4f$, $4d5p$, and $4f5g$, among others. While the energy of the resonance is reduced to 4.8695 eV (or $-0.030\,04$ a.u. below the Na^+ threshold), these calculations find that the configurations involving $4d$ and/or $4f$ orbitals have only very small weightings in the configuration representation for this resonance. We conclude that despite the breadth of this resonance feature, it is not a core-excited shape resonance.

IV. DISCUSSION

Very few predictions for the ^1P doubly excited state resonances of Na^- have been reported, although our present re-

TABLE I. $^1P^o$ autoionizing levels of Na^-.

Present results			Stewart *et al.* [20]	Zatsarinny *et al.* [34]	Haeffler *et al.* [25]
E_+ (a.u.) [a]	E_{3s} (eV) [b]	$\hbar\omega$ (eV)	$\hbar\omega$ (eV)	$\hbar\omega$ (eV)	$\hbar\omega$ (eV)
				2.64	
−0.061 46	3.4665	4.0145	4.122	4.10	
				4.12	
				4.16	
−0.051 10	3.7487	4.2966		4.30	
−0.037 90	4.1078	4.6557			
−0.034 93	4.1886	4.7365			4.73268(56)
−0.032 29	4.2605	4.8084			4.80696(4)
−0.031 70	4.2763	4.8243			4.82647(18)
−0.031 30	4.2874	4.8353			4.83132(16)
−0.030 04	4.3216	4.8695		4.89	

[a]Energy with respect to the Na^+ threshold.
[b]Energy with respect to the Na($3s$) ground state.

sults show that there exists a rich structure of resonances below the first few thresholds of Na. We compare our predicted energies with results of Refs. [20,25], and [34] in Table I. Stewart *et al.* [20] find a single $^1P^o$ resonance below the Na($3d$) threshold, in agreement with our results, but their energy position is significantly higher than ours, owing to the different (i.e., standard and nonstandard) projection operator methods used to obtain these results, as discussed in Sec. III B. Only two of the six $^1P^o$ resonances that are predicted by Zatsarinny *et al.* [34] agree with the present predictions. Very recently, Haeffler *et al.* [25] gave energies and widths for the resonances lying between the Na($5s$) and Na($4d$) thresholds obtained by fitting results of their partial cross-section measurements to the Shore profile formulas [41]. The agreement between our calculated energies and the fitted experimental energies is very good, as might be expected from the excellent agreement between the predicted and measured Na($4s$) partial cross-section results shown in Fig. 8.

Since our analyses using the nonstandard projection operator method indeed characterize all features in the photodetachment spectra (both in the partial cross sections and in the β parameters), we are confident that this method provides a better description of the doubly excited state wave functions, including those responsible for core-excited shape resonances. In all cases, doubly excited states show strong configuration mixing, reflecting the complexity of electron correlations in this system.

The analysis in the preceding section shows that the symmetry notations for the doubly excited states for H^- still hold, at least approximately, for Na^- in this energy range. By comparing the wave-function density plots for corresponding doubly excited states of H^- and Na^-, it is evident that the nodal structure in Na^- is not as sharp as in H^-, reflecting a mixing of different angular symmetries, which we attribute to the non-Coulomb Na^+ core that the excited pair of electrons in Na^- see. Even though these mixing effects do not change the correlation pattern of the wave functions dramatically, the effects on the spectra are significant. Spectra in this energy region clearly show the prominence of ''−'' type resonances, in contrast to the case of H^-, where ''+'' type doubly excited states dominate the spectra and ''−'' type states only appear as extremely narrow resonances. In the spectra of Na^- photodetachment, we even find a resonance whose probability density has a nodal line in θ_{12} in violation of the propensity rules [6,7] developed for H^- photodetachment spectra. Such resonances have not been observed in the spectrum of H^-.

Relative to the respective double detachment thresholds of Li^- and Na^-, corresponding highly excited, two-electron states are expected to appear at similar energies in the two spectra, even though Na has a different ordering of excited atom thresholds. Indeed, these two spectra show parallel resonance structures, i.e., states with similar probability densities, having similar angular and radial correlation patterns, are found. However, there are some differences due to the different ordering of the excited thresholds, reflecting different core effects. For example, while the most prominent resonance structures appear between the ns and $(n-1)d$ thresholds in Na^- spectra, they appear between the ns and np thresholds in Li^-. This fact can be related to the polarizabilities of the excited states of Li and Na.

Polarizabilities of the excited states play an important role in the formation of resonances since they dominate the long-range interaction between the neutral atom and the additional electron. However, positive polarizability is not the most important criterion for the formation of a two-electron resonance; rather an attractive effective interaction including electron correlation is. In the Li^- spectrum [10,12], there is a resonance series converging to each of the excited state thresholds that has a positive polarizability. But no resonances were found to be associated with those thresholds having negative polarizabilities. While the most prominent resonance series are those converging to the np thresholds, there are less prominent resonance series converging to the nd thresholds, except for $3d$. All of these thresholds have positive polarizabilities. However, there is only one resonance associated with the Na($5p$) threshold, which has a negative polarizability. An effective potential point of view allows one to understand this result. This formation of a doubly excited resonance indicates an attractive effective potential, at least at short range. However, the repulsive long-range interaction may produce only a narrow potential well, thus reducing the number of bound states in the effective

potential. Such reasoning may explain the sole resonance below the Na($5p$) threshold.

An interesting common feature appears in the first resonance appearing just above each of the Na($4s$) and Na($5s$) thresholds. Both doubly excited states have strong contributions from a configuration having either a $4s$ or a $5s$ orbital. Thus both resonances exhibit shape-resonance-type behavior. The breadth of each of these resonances and the prominence of the $4s$ and $5s$ partial cross sections support this observation. Another piece of information comes from the wave-function density plots in hyperspherical angular variables, where a weak peak near α equal to 0 (or $\pi/2$) indicates that one electron is relatively far away from the nucleus. On the other hand, both resonances also have strong contributions from the configurations associated with bound orbitals, which is reflected by the dominance of the angular symmetry character of the corresponding Feshbach resonances in H^-. This is another example showing that the correlation in Na^- is rather complex, that all configurations are strongly mixed, and thus a single configuration is no longer a proper label for these doubly excited states.

V. CONCLUSIONS

We have presented detailed theoretical studies for Na^- photodetachment over the energy region from the Na($3s$) threshold to the Na($5p$) threshold (i.e., for 0.548 eV$\leqslant\hbar\omega\leqslant$5 eV). Spectra of both the partial cross sections and the photoelectron asymmetry parameter β for the process $Na^- + \gamma \rightarrow Na(3p) + e^-$ are provided. We have also analyzed all doubly excited resonances in the energy region indicated using a nonstandard projection operator method that enables us to characterize not only Feshbach resonances but also those states having properties of core-excited shape resonances. In the energy region between the Na($4s$) and Na($3d$) thresholds, we find a single doubly excited state dominates the partial cross section and the β parameter for the process $Na^- + \gamma \rightarrow Na(3p) + e^-$. In the energy region from the vicinity of the Na($5s$) threshold to the Na($4f$) threshold, we find there are five resonances, having three different kinds of radial and angular symmetry, which determine both the structure in the partial cross sections and that in the β parameter corresponding to the Na($3p$) state. Below the Na($5p$) threshold, we have identified an additional ''$-$'' type resonance state even though the Na($5p$) state has a negative polarizability. In many cases, our predictions are either the first or else the first to characterize the doubly excited resonance states in this energy region of the Na^- photodetachment spectrum.

Throughout the paper, we have further provided insights into the resonance features appearing in the spectra. It is shown that configurations are strongly mixed, indicating the impropriety of single configuration designations. Mirroring effects among the partial cross sections have been understood as a common resonance feature at high levels of excitation of the residual atom [26] and examples are noted here. The nonhydrogenic nature of the Na^+ core leads to prominence of doubly excited resonances that are absent in H^- photodetachment spectra, as was also found in analyses of the Li^- photodetachment spectrum [10,12,13]. Similarities and differences of the resonance structures in the H^-, Li^-, and Na^- photodetachment spectra below particular thresholds are discussed and related to different threshold orderings and different atom polarizabilities. Although the appearance of resonance series is sensitive to the asymptotic interaction of the pair of correlated electrons due to polarization, the more complicated short-range behavior of the electron-electron correlation is the key to understanding the two-electron dynamics.

We have compared our work on the Na^- photodetachment spectrum and on the important $^1P^o$ doubly excited states in its spectrum with all prior theoretical and experimental work known to us. Detailed comparisons are given with the work of Moores and Norcross [19], whose four-state close-coupling calculation fairly accurately describes the Na^- photodetachment cross section below the Na($3p$) threshold. Our predictions for the Na($4s$) partial cross section between the Na($5s$) and Na($4f$) thresholds are in excellent agreement with the recent measurements of Haeffler *et al.* [25] presented in the following paper.

ACKNOWLEDGMENTS

We thank G. Haeffler, D. Hanstorp, I. Yu. Kiyan, and D. Pegg for useful discussions and for providing us with the experimental data of Ref. [25] prior to publication. We also thank P.D. Burrow for discussions concerning electron-sodium collisions. This work has been supported in part by the U.S. Department of Energy, Office of Basic Energy Sciences, under Grant No. DE-FG-03-96ER14646.

[1] D. R. Herrick, Phys. Rev. A **12**, 413 (1975); Adv. Chem. Phys. **52**, 1 (1983).

[2] C. D. Lin, Phys. Rev. A **29**, 1019 (1984); Adv. At. Mol. Phys. **22**, 77 (1986).

[3] J. M. Feagin and J. S. Briggs, Phys. Rev. Lett. **57**, 984 (1986); Phys. Rev. A **37**, 4599 (1988).

[4] J. M. Rost, R. Gersbacher, K. Richter, J. S. Briggs, and D. Wintgen, J. Phys. B **24**, 2455 (1991).

[5] P. G. Harris, H. C. Bryant, A. H. Mohagheghi, R. A. Reeder, H. Sharifian, C. Y. Tang, H. Tootoonchi, J. B. Donahue, C. R. Quick, D. C. Rislove, W. W. Smith, and J. E. Stewart, Phys. Rev. Lett. **65**, 309 (1990).

[6] H. R. Sadeghpour and C. H. Greene, Phys. Rev. Lett. **65**, 313 (1990); H. R. Sadeghpour, Phys. Rev. A **43**, 5821 (1991); H. R. Sadeghpour, C. H. Greene, and M. Cavagnero, *ibid.* **45**, 1587 (1992); H. R. Sadeghpour and M. Cavagnero, J. Phys. B **26**, L271 (1993).

[7] J. M. Rost and J. S. Briggs, J. Phys. B **23**, L339 (1990); A. Vollweiter, J. M. Rost, and J. S. Briggs, *ibid.* **24**, L115 (1991); J. M. Rost and J. S. Briggs, *ibid.***24**, 4293 (1991); J. M. Rost, J. S. Briggs, and J. M. Feagin, Phys. Rev. Lett. **66**, 1642 (1991).

[8] J. Z. Tang, Y. Wakabayashi, M. Matsuzawa, S. Watanabe, and I. Shimamura, Phys. Rev. A **49**, 1021 (1994); J. Z. Tang and I. Shimamura, *ibid.* **51**, R1738 (1995).

[9] See, for example, Y. K. Ho, Phys. Rev. A **45**, 148 (1992), and references therein.
[10] C. Pan, A. F. Starace, and C. H. Greene, J. Phys. B **27**, L137 (1994).
[11] E. Lindroth, Phys. Rev. A **52**, 2737 (1995).
[12] C. Pan, A. F. Starace, and C. H. Greene, Phys. Rev. A **53**, 840 (1996).
[13] C. N. Liu and A. F. Starace, Phys. Rev. A **58**, 4997 (1998).
[14] U. Berzinsh, G. Haeffler, D. Hanstorp, A. Klinkmüller, E. Lindroth, U. Ljungblad, and D. J. Pegg, Phys. Rev. Lett. **74**, 4795 (1995).
[15] U. Ljungblad, D. Hanstorp, U. Berzinsh, and D. J. Pegg, Phys. Rev. Lett. **77**, 3751 (1996).
[16] G. Haeffler, I. Yu. Kiyan, D. Hanstorp, and D. J. Pegg, Phys. Rev. A **57**, 2216 (1998).
[17] Yu. V. Moskvin, Teplofiz. Vys. Temp. **3**, 821 (1965) [Sov. Phys-High Temp. **3**, 765 (1965)].
[18] T. L. John and A. R. Williams, J. Phys. B **5**, 1662 (1972).
[19] D. L. Moores and D. W. Norcross, Phys. Rev. A **10**, 1646 (1974).
[20] R. F. Stewart, C. Laughlin, and G. A. Victor, Chem. Phys. Lett. **29**, 353 (1974).
[21] M. Ya Amusia, C. F. Gribakin, V. K. Ivanov, and L. V. Chernysheva, J. Phys. B **23**, 385 (1990).
[22] R. Moccia and P. Spizzo, Nuovo Cimento D **13**, 757 (1991).
[23] T. A. Patterson, H. Hotop, and W. C. Lineberger (unpublished). Results shown in Fig. 6 of Ref. [19].
[24] H. J. Kaiser, E. Heinicke, R. Rackwitz, and D. Feldmann, Z. Phys. **270**, 259 (1974).
[25] G. Haeffler, I. Yu. Kiyan, D. Hanstorp, B. J. Davies, and D. J. Pegg, following paper, Phys. Rev. A **59**, 3655 (1999).
[26] C. N. Liu and A. F. Starace, Phys. Rev. A **59** R1731 (1999).
[27] A. R. Johnston and P. D. Burrow, Phys. Rev. A **51**, 406 (1995).
[28] U. Fano and C. M. Lee, Phys. Rev. Lett. **31**, 1573 (1973).
[29] P. F. O'Mahony and C. H. Greene, Phys. Rev. A **31**, 250 (1985); C. H. Greene and L. Kim, *ibid.* **36**, 2706 (1987); C. H. Greene, in *Fundamental Processes of Atomic Dynamics*, edited by J. S. Briggs, H. Kleinpoppen, and H. O. Lutz (Plenum, New York, 1988), pp. 105-127.
[30] W. R. Johnson, D. Kolb, and K.-N. Huang, At. Data Nucl. Data Tables **28**, 333 (1982).
[31] C.E. Moore, *Atomic Energy Levels*, Natl. Bur. Stand. (U.S.) No. NSRDS-NBS35 (U.S. GPO, Washington, DC, 1971).
[32] See, e.g., U. Fano and A. R. P. Rau, *Atomic Collisions and Spectra* (Academic, New York, 1986), pp. 76–77.
[33] M. Eyb and H. Hofmann, J. Phys. B **8**, 1095 (1975).
[34] O. I. Zatsarinny, V. I. Lengyel, E. P. Sabad, and I. I. Cherlenyak, Izv. Akad. Nauk SSSR, Ser. Fiz. **50**, 1377 (1986).
[35] T. A. Patterson, H. Hotop, A. Kasdan, D. W. Norcross, and W. C. Lineberger, Phys. Rev. Lett. **32**, 189 (1974).
[36] D. L. Moores and D. W. Norcross, J. Phys. B **5**, 1482 (1972).
[37] A. L. Sinfailam and R. K. Nesbet, Phys. Rev. A **7**, 1987 (1973).
[38] M. Eyb, J. Phys. B **9**, 101 (1976).
[39] U. Fano and J. W. Cooper, Phys. Rev. **137**, A1364 (1965); Rev. Mod. Phys. **40**, 441 (1968).
[40] P. F. Gruzdev, G. S. Soloveva, and A. I. Sherstyuk, Opt. Specktrosk. **71**, 888 (1991) [Opt. Spectrosc. **71**, 513 (1991)].
[41] B. W. Shore, Phys. Rev. **171**, 43 (1968).